




Modelling of the burial and thermal histories of Jurassic-Cretaceous total petroleum system, Southeastern Tunisia

D. Tanfous¹ · F. Dhahri^{2,3}  · H. Gabtni⁴ · M. Saidi⁵ · M. Soussi¹

Received: 5 September 2021 / Accepted: 13 May 2022 / Published online: 23 June 2022
© The Author(s), under exclusive licence to Universidad Complutense de Madrid 2022

Abstract

The Jeffara basin in Southeastern Tunisia is a part of a wide Jurassic-Cretaceous petroleum system extending from the Saharan platform to the Pelagian province in eastern Tunisia and northwestern Tripolitania. In this petroleum province, El Bibane and Ezzaouia offshore fields were discovered in 1982–1986 as NE-SW folded structural traps. Their present-day accumulations are stuck within the Cenomanian carbonates of the Zebbag Formation and the Kimmeridgian marine clastic sequence of the Mrabtime Member respectively. The tectono-thermal evolution and the burial history modelling of the source rocks using wells and gravity data allowed us to identify the relationship between the deep crustal structure of the Jeffara basin and the evolution of its petroleum systems. The gravity data analysis using inversion method shows that the Jeffara basin is associated with a regional major NW–SE positive gravity anomaly related to about 5 km crustal thinning from west to East. This crustal thinning setting have locally controlled the burial histories of Ezzaouia and El Bibane oil fields.

Keywords Jeffara basin · Gravity data · Crustal thinning · Thermal subsidence · Hydrocarbon maturation

Resumen

La cuenca de Jeffara en el sureste de Túnez forma parte de un amplio sistema petrolífero de edad Jurásico-Cretácica que se extiende desde la Plataforma Sahariana hasta la provincia de Pelagia en el este de Túnez y el noroeste de Tripolitania. En esta provincia petrolera, los campos offshore El Bibane y Ezzaouia fueron descubiertos en 1982–1986 como trampas estructurales en pliegues NE-SW. Sus acumulaciones actuales se encuentran respectivamente en los carbonatos cenomanienses de la Formación Zebbag y en las sucesiones clásticas marinas kimmeridgienses del Miembro M'rabtime. La modelización de la evolución tectono-termal y del enterramiento de las rocas madre, realizada a partir de datos de sondeos y gravimétricos, ha permitido identificar la relación entre la estructura cortical profunda de la cuenca de Jeffara y la evolución de sus sistemas petrolíferos. El análisis de los datos gravimétricos utilizando el método de inversión muestra que la cuenca de Jeffara está asociada con una importante anomalía gravimétrica positiva, con orientación NW-SE, y relacionada con un adelgazamiento de la corteza de aproximadamente 5 km desde el oeste hacia el este. Este adelgazamiento cortical ha controlado la evolución del enterramiento en los campos petrolíferos de Ezzaouia y El Bibane.

Palabras clave Cuenca de Jeffara · datos gravimétricos · adelgazamiento cortical · subsidencia térmica · maduración de hidrocarburos

✉ F. Dhahri
feriddhahri@yahoo.fr

¹ Département de Géologie, Faculté Des Sciences de Tunis, Université Tunis El Manar, EL Manar II, Tunis, Tunisie

² Laboratoire Géodynamique, Géomatériaux Et Géo-Numérique, Faculté Des Sciences de Tunis, Université Tunis El Manar, EL Manar II, Tunis, Tunisie

³ Faculté Des Sciences de Gafsa, Département Des Sciences de La Terre, Université de Gafsa, Gafsa 2011, Tunisie

⁴ Laboratoire de Géoresources, Centre de Recherches Et Des Technologies Des Eaux (CERTe), Soliman, Tunisie

⁵ Entreprise Tunisienne Des Activités Pétrolières (ETAP), 54 Avenue Mohamed V, Tunis, Tunisie

1 Introduction

Southeastern Tunisia (Fig. 1) rises many petroleum challenges due to, in part, the presence of proven source rocks (Jurassic and Early Cretaceous series) (Ben Ferjani et al., 1990; Bishop, 1975; Klett, 2001) and its complex structural heritage. The petroleum exploration southward the Gulf of Gabes led to the discoveries of Ezzaouia and El Bibane oil fields (Fig. 2) within the Jurassic and the Middle Cretaceous series (Ben Ferjani et al., 1990; Touati et al., 1998) and highlighted also several good potential undrilled traps (pinch outs, tilted blocks and salt structures flanks).

During Late Triassic-Liassic, the E–W rifting phase widened the Tethyan realm and engendered several NNW–SSE to NW–SE extensional structures in the Gulf of Gabes and Jeffara basin (Bouaziz et al., 2002; Gabtni et al., 2009a, 2009b; Ghedhoui et al., 2016; Patriat et al., 2003). Subsequently, two main marine domains were structured: the relatively shallow area to the west of Gabes and Djerba, and the deep area near the subsiding blocks of Ezzaouia–El Bibane to the East (Touati et al., 1998; Lazzez et al., 2014) (Fig. 1). The NE–SW extension during Middle Jurassic–Late Cretaceous reactivated the inherited NNW–SSE and NW–SE faults and engendered NW–SE oriented high and low zones in the Jeffara basin (Bouaziz et al., 2002; Patriat et al., 2003).

The tectonic subsidence in the Jeffara basin was seemingly associated to the Mesozoic episodes of rifting occurred in passive margin conditions. However, it was aborted by an E–W compressive event related to the collision of European and African plates during Aptian–Albian times (Bouaziz et al., 2002, 2015; Patriat et al., 2003). This compressional tectonic engendered some reverse slips of several ancient normal faults in the Jeffara basin and the inversion of the subsiding Ezzaouia–El Bibane areas (Touati et al., 1998) with partial erosion of Lower Cretaceous levels within uplifted blocks (Touati et al., 1998).

The aim of this work is to precise the relationship between the deposition of Jurassic–Cenozoic series, their thermal subsidence and the crustal structure underneath that controlled tectonic subsidence with emphasize of the Jurassic–Cretaceous total petroleum system near Ezzaouia and El Bibane fields in southeastern Tunisia (Fig. 2). In fact, the study area is tectonically complex since it is located to the east of the Hercynian E–W Arch of Telemzane–Dahar and within the Jeffara basin affected by crustal NW–SE normal faults engendering a gradual NE-trending slope of the area toward the Ashtart–Tripolitania basin, offshore, and recording also the shortening of the Alpine orogeny. Therefore, to achieve the goals of this work available data from industry wells (chronostratigraphy, thickness and depth of crossed formations, Bottom Hole Temperature (BHT)), satellite gravity data and previous literature are gathered. Chemical analysis (TOC, Rock–Eval, Hydrogen Index (HI), Oxygen

Index (OI), Production Index (PI) and vitrinite reflectance) of samples taken from reservoir levels cores were completed for this work and used with well data to perform the modeling of the burial and thermal histories by means of Genex software. Results are discussed in light of the geodynamic evolution, tectonic history and petroleum exploration of the study area published in previous literature.

2 Geological setting

Southern Tunisia is occupied by the so-called Saharan platform geologically made of three main domains; the Ghadames Basin, to the south, straddling southern Tunisia, northwestern Libya and eastern Algeria, the Hercynian E–W Arch of Telemzane–Dahar (Busson, 1967), and the Jeffara basin affected by NW–SE normal faults engendering a gradual slope of the area toward the northeast, offshore. The Saharan platform is made of Mesozoic series resting uncomfortably over Paleozoic strata, however toward the northeast, Cenozoic deposits occupy the area extending from the coastal maritime Jeffara to the collapsed Tripolitania Basin offshore (Benton et al., 2000; Bodin et al., 2010).

Quaternary to Permian series in Jeffara basin have been recognized in outcrop, however ante-Permian to Precambrian ones were studied using well cores of petroleum exploration wells (Ben Ferjani et al., 1990; Touati et al., 1998). In southern Tunisia, Paleozoic series are dominantly made of clastic continental sediments. The Lower to Middle Triassic series are shallow marine carbonates. These series are not reached by the industry wells in the study area since the latter were bottomed in the Upper Triassic and led to establish the synthetic chronostratigraphy chart of Fig. 3. The Late Triassic strata are mainly evaporitic and they exceed 2000 m thick. The Jurassic series are of shallow shelf to sabkha environments with an average total thickness of ~1300 m. The Middle Jurassic series are made of shales interbedded with anhydrites and dolomites (Ben Ferjani et al., 1990; Touati et al., 1998). They exhibit clear prevalence of evaporitic conditions toward the south, whereas, further to the north, their facies is dominantly dolomitic. Their upper part includes two intervals with good reservoir qualities acknowledged as the Techout (clastic) and Smida (sands and dolomites interbedded with shale) members. The latter exhibits significant thickness variation from 85 m in P2 to 280 m in P3. The Upper Jurassic series are made of a shaly sequence intercalated with several sandstone horizons acknowledged as Mrabtime member. This member reaches 450 m in P3 well and it is sealed by an efficient evaporitic horizon. It is a proven onshore oil-bearing sandstone reservoir with good reservoir qualities in Ezzaouia field (Soussi et al., 2004). Beach or tidal flat sands may provide its lateral continuity in southern Gulf of Gabes.

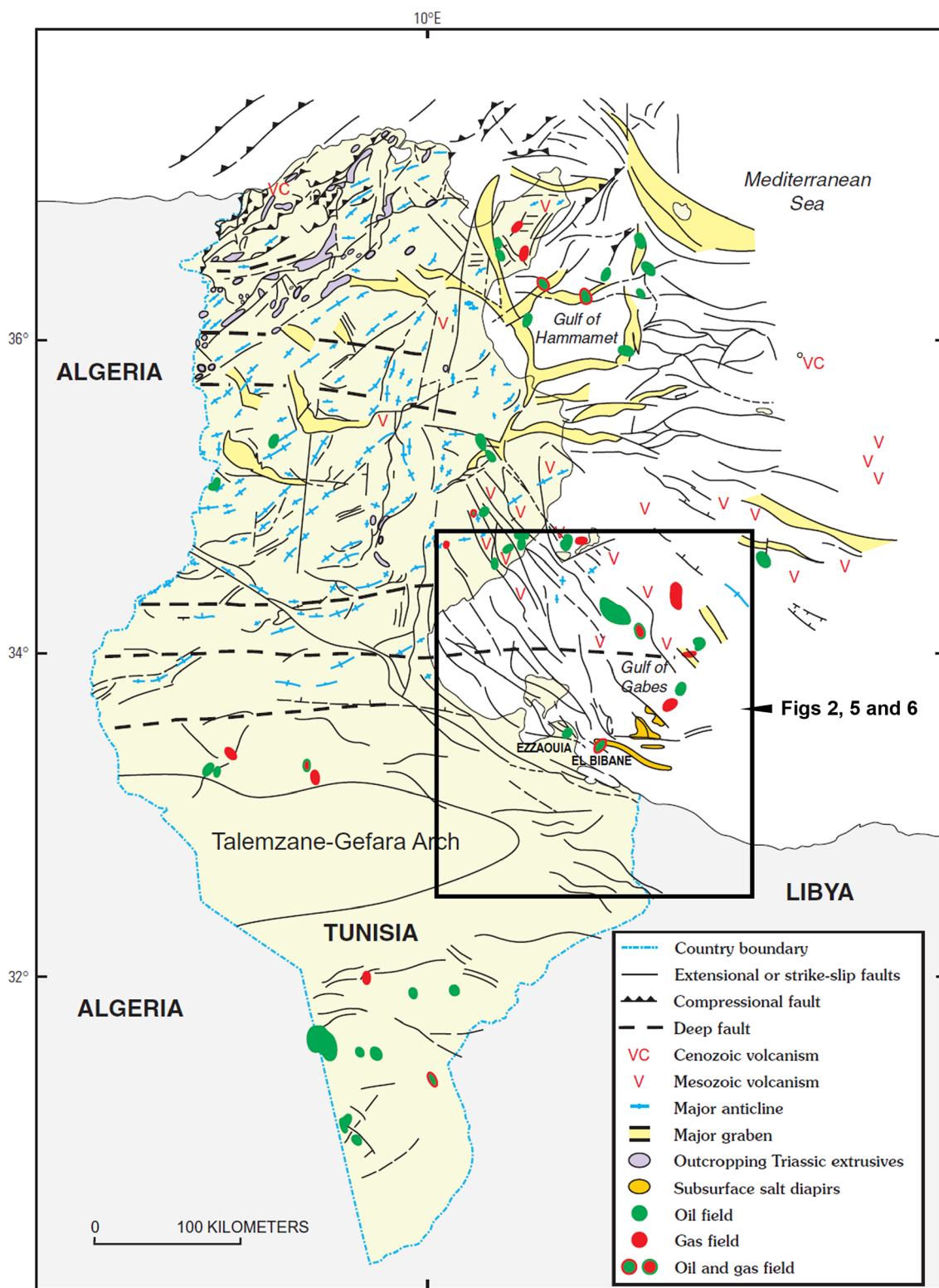


Fig.1 Regional structural sketch of Tunisia and surrounding areas (in Klett, 2001) with location of the study area

The Cretaceous series are 1400 m thick in average. They begin with the two clastic sequences of the Meloussi (Lower Valanginian-Lower Hauterivian) and Boudinar Formations

(Upper Hauterivian-Lower Barremian) followed by the anhydritic sequence of Bouhedma Formation (Lower-Middle Barremian). Another clastic cycle occurred during the

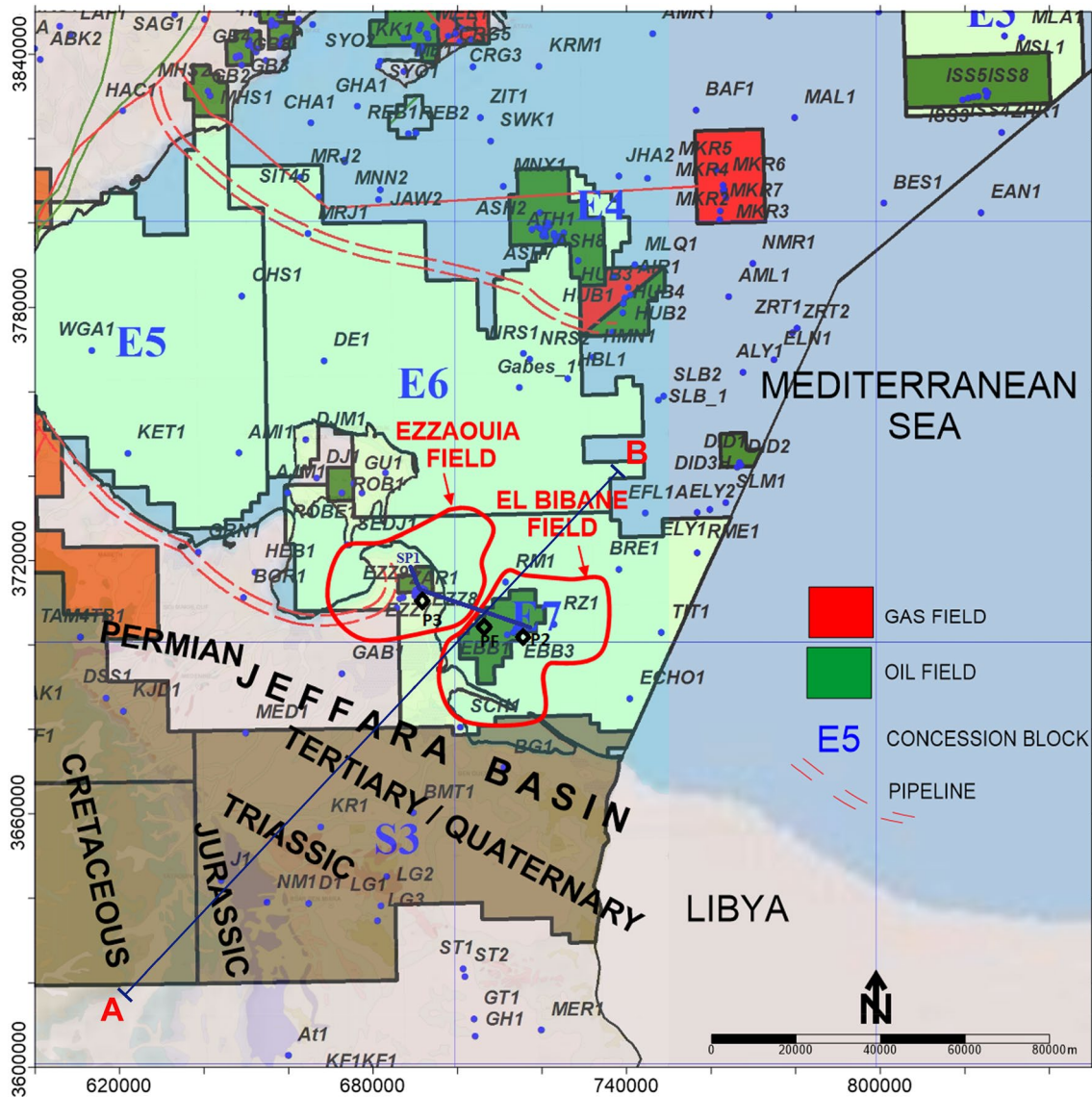


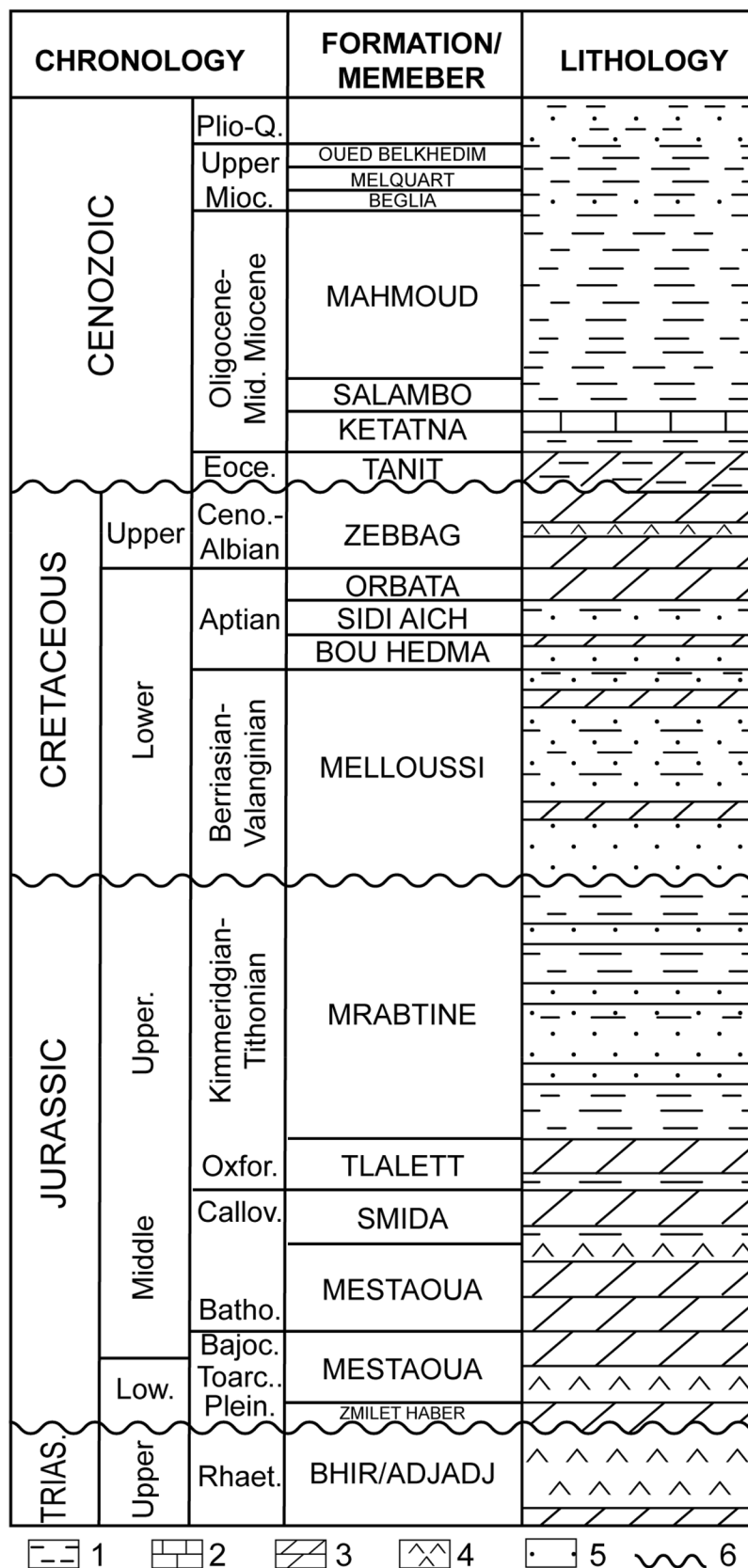
Fig. 2 Geological and hydrocarbon setting of the study area (Ben Haj Ali et al., 1985 and Ben Ferjani et al., 1990). A–B: location of the NE-SW density variation section of Fig. 7

Upper Barremian and gave the sandy Sidi Aich Formation (Ben Ferjani et al., 1990; Touati et al., 1998) followed by the transgressive carbonate sequence of Zebbag Formation encompassing a dolomitic middle member with good primary porosity enhanced by fracturing and good permeability and it is sealed by a thick sequence of anhydrites. This reservoir/seal combination is the main trapping system of the El Bibane field (Fig. 4). During the Turonian–Maastrichtian, continuous transgressive conditions led to the migration of the marine domain towards the South. However, these transgressive series are eroded in Ezzaouia field where the Cenozoic sediments lay directly over the reservoir of Middle Zebbag Formation according to the so-called top Cretaceous unconformity (Fig. 4).

During the Cenozoic, a sequence of about 1400 m thick has been deposited in the eastern part of the region. This sequence includes an Eocene continental to shallow marine deposition (sands, anhydrites and dolomites) followed by a carbonate series Oligocene to Early Miocene in age (Ketatna Formation). During the Middle Miocene were deposited the limestones of Mahmoud Formation, followed by the deltaic sandstones of Beglia Formation and topped by a marine sequence of limestones (Melquart Formation) underlining the end of Miocene. The Messinian series are of regressive conditions and Pliocene series are made of marine clays.

The geodynamic evolution of the area was discussed in several works (e.g. Bodin et al., 2010; Gabtni et al.,

Fig. 3 Synthetic chronostratigraphy chart of Ezzaouia-El Bibane area. (1) shales, (2) limestones, (3) dolomites, (4) evaporites, (5) sandstones/detrital facies, (6) unconformity



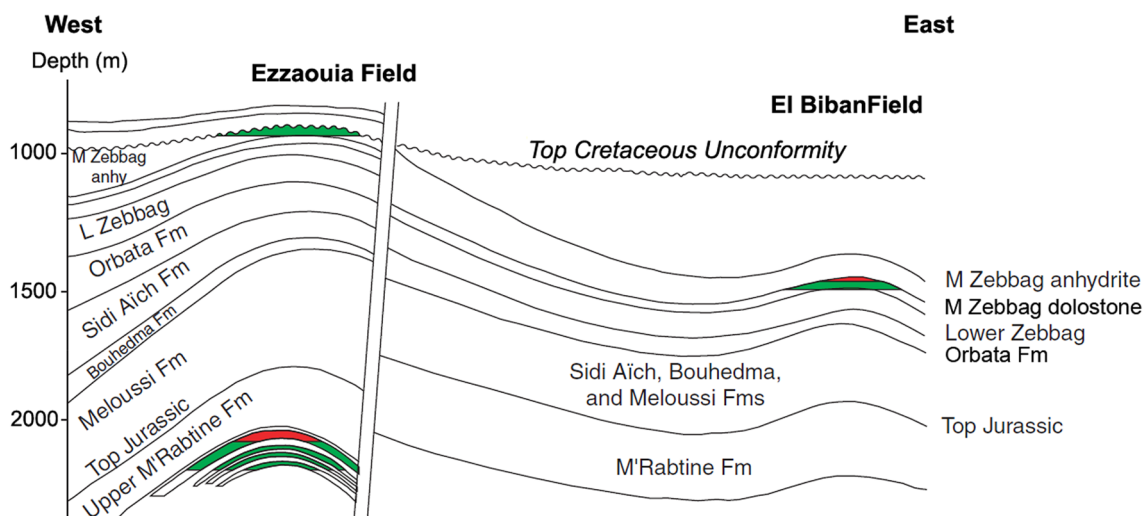


Fig. 4 Synthetic geoseismic cross-section along the Ezzaouia and El Bibane oil fields (Klett, 2001)

2009a, 2009b; Raulin et al., 2011) highlighting that its structure is the result of some key events recorded from Paleozoic to Neogene times. After the Hercynian orogeny responsible for the uplift of the Telemzane-Dahar Arch followed by regional erosion and recorded as the so-called Hercynian unconformity Busson, 1967, extensional tectonics are recorded for the Permian–Triassic times and continued until Upper Jurassic–Lower Cretaceous. These extensional events related to Tethys rifting produced a series of NW trending normal faults associated with magmatism and salt pillows especially during Triassic times. During Aptian period –onset of the Alpine orogeny– local uplift in the Ezzaouia area resulted in the initiation of basin inversion (Fig. 4). The synthetic section of Fig. 4 (internal report of the Entreprise Tunisienne des Activités Pétrolières (1999) in Klett (2001)), shows that the local uplift of the Ezzaouia field is controlled by a sub-vertical deep faults. Later on, a regional wrench and a compressional event Santonian in age engendered numerous E-W oriented right lateral strike slip faults resulting in the formation of NE-SW trending folds and NW–SE oriented diapiric salt walls. Folds are mainly asymmetric with southeast steep flanks affected by reverse faults (Touati et al., 1998). During Eocene–Oligocene period a moderate compression enhanced compressional structures. A NE–SW extension occurred during Late Miocene–Early Pliocene times and has reactivated inherited Mesozoic faults (Booth-Rea et al., 2018). The latest significant tectonic event is post-Villafranchian in age and occurred as NNW–SSE compression. It accentuated the ancient NE-SW Cretaceous folds and led to the emersion of some Late Cretaceous (Santonian) structures mainly affected by deep E-W dextral strike slip faults (Ben Ferjani et al., 1990; Touati et al., 1998).

3 Methods and data

Data used in this work are gathered from three industry wells, gravity and published literature. Well data (Tables 1, 2, 3, 4, 5) included available information's from final well reports such as chronostratigraphy, thickness and depth of crossed formations, implicit gaps and amounts of erosion, BHT and also chemical data derived from core samples analysis such as COT, Rock–Eval pyrolysis, HI, OI, PI and vitrinite reflectance data. The Rock–Eval pyrolysis was performed in the Organic Geochemistry Laboratory of the "Entreprise Tunisienne d'Activités Pétrolières" (ETAP). During the analysis, the amounts of hydrocarbons, kerogen and CO₂ present in the sample are volatilized and recorded respectively as three peaks S1, S2 and S3. The residual carbon is recorded as S4 (Espitalié et al., 1985). HI, OI and PI are deduced from S1, S2 and S3 peaks as described by (Espitalié et al., 1977). To calculate thermal history for the studied wells bottom-hole temperatures, vitrinite reflectance data, and assumed paleo-surface temperatures are the input data used by Genex software to calibrate thermal models. Thermal calibrations were carried out for P1, P2 and P3 wells using Genex software and the best adjustments between the measured and calculated values were obtained for a heat-flow varying between 60 and 65 mW/m². The bottom-hole temperatures were taken from available records on log headers of the individual wells used in modeling or from headers of wells nearby. Heat-flow values are used for the burial-history reconstructions (Tables 3, 4, 5). The present-day heat-flow values at the base of the stratigraphic column of each modeled well was determined using Genex1D software by calibrating with the corrected downhole temperatures and the present-day and assumed paleo-surface temperatures. As considered

Table 1 Data used to generate burial-history curves for P1 well

Series, Unit, Event	Age (m.y)	Top depth (m)	Eroded (m)	Lithology
<i>Post Vill. (Unconformity)</i>	0,8		100	
Upper Segui (<i>hiatus</i>)	2		100	ss 45, sh 40, lms 10, anh 5
Segui	3	0		ss 45, sh 40, lms 10, anh 5
Pliocene (<i>Unconformity</i>)	5,5		100	
Oued bel khedim (<i>hiatus</i>)	6		50	sh 55, ss 20, anh 15, lms 10
Melquart (<i>hiatus</i>)	8		50	sh 55, ss 20, anh 15, lms 10
Upper Beglia		60		sh 65, ss 20, lms 10, anh 5
Lower Beglia	15	176		ss 60%, sh 35%, lms 5%
Mahmoud	16	253		sh 50%, lms 30%, ss 20%
Salambo	17	466		sh 50, mar 30, lms 15, ss 5
Ketatna	34	770		lms 50%, sh 30%, mar 20%
Oligocene (<i>Unconformity</i>)	36		250	
Upper Tanit (<i>hiatus</i>)			250	sh 50, ss 25, dol 15, mar 10
Lower Tanit	55	899		sh 40, ss 35, dol 15, mar 10
Santonien (<i>Unconformity</i>)	83		500	
Upper/Mid. Aleg (<i>hiatus</i>)	86		200	sh 65, mr 20, lms 15
Lower Aleg (<i>hiatus</i>)	90,5		200	lms 35, anh 25, sh 20, dol 20
Beida (<i>hiatus</i>)	91		100	anh 70%, dol 20%, sh 10%
Guettar	91,5	943		dol 90%, anh 10%
Zebbag	95	1000		dol 70%, anh 20%, sh 10%
Albien (<i>Unconformity</i>)	108		150	
Upper Orbata (<i>hiatus</i>)	113		150	dol 50, ss 30, sh 20
Lower Orbata	115	1242		dol 50, ss 40, sh 10
Sidi Aïch	120	1274		ss 55, sh 30, dol 10, anh 5
Upper Bouhedma	123	1374		dol 50, sh 20, anh 15, ss 15
Lower Bouhedma	127	1459		sh 40, ss 30, dol 20, anh 10
Bou Dinar	130	1755		ss 75, sh 15, dol 10
<i>Lw. Cretaceous (Unconformity)</i>	145			
Mrabtine	155	1890		dol 35, sh 30, lms 20, anh 15
Tlalett	160	2340		

ss = sandstone, sh = shale, lms = limestone, anh = anhydrite, dol = dolomite, mr = marl

in other studies (e.g. Roberts et al., 2005), the estimated amounts of erosion, which could affect the calibration, were left unchanged. Heat flow may also vary through time and it was not necessary to make assumptions about when changes of heat flow occurred or the extent to which it changed through time. In practice, performing model with a constant heat flow through time resulted in an acceptable match of calculated R_0 values, as determined by EASY% R_0 (Sweeney & Burnham, 1990) with the measured R_0 values.

The commercial Genex1D software licensed to the Reservoir Department of the ETAP was used to perform quantitative 1D modeling of burial history and thermal maturity for the three wells P1, P2 and PF. The input parameters for modelling include lithology of strata, thickness, age, hiatus and heat flow. These wells were chosen because they were drilled to a depth that penetrated a significant part of the

geologic section of interest (Jurassic series). In addition, they are located within areas of different geologic settings in the studied province and they have measured vitrinite reflectance and downhole temperature data to aid in calibrating maturation models (Table 6). Tables 3, 4, 5 show the age, thickness and generalized lithological data used to establish the burial-history curves.

The satellite gravity data used for this study were obtained from the “Bureau Gravimétrique International” (BGI). The regional Free-air and Bouguer gravity anomaly grids (averaged over 2,5 arc-minute by 2,5 arc-minute) are computed at BGI from the EGM2008 spherical harmonic coefficients (Pavlis et al., 2008). The Bouguer corrections computed at regional scales are obtained using the FA2BOUG code developed by Fullea et al. (2008). The topographic correction is applied up to a distance of 167 km using the 1 arc-minute by 1 arc-minute ETOPO1 Digital.

Table 2 Smida source Rock Pyrolysis analyses of P1 and P2 wells

Well name	Depth (m)	TOC	S1 (mg/g)	S2 (mg/g)	S3 (mg/g)	HI	OI	IP	Tmax (°C)
P1	2784	0,42	0,07	0,32	0,22	76	52	0,18	443
	2798	0,25	0,05	0,19	0,15	76	60	0,21	445
	2820	0,26	0,05	0,2	0,19	77	73	0,2	440
	2826	0,34	0,07	0,28	0,18	82	53	0,2	437
	2832	0,31	0,07	0,26	0,26	84	84	0,21	432
	2842	0,41	0,11	0,47	0,33	115	80	0,19	434
P2	2815	1,06	0,92	3,74	0,43	353	41	0,2	441
	2820	1,06	0,55	4,39	0,44	414	42	0,11	442
	2825	0,66	0,42	2,43	0,37	368	56	0,15	441
	2830	1,01	0,45	4,16	0,3	412	30	0,1	448
	2840	1,4	0,82	5,78	0,42	413	30	0,12	448
	2845	1	0,87	5,08	0,37	508	37	0,15	452
	2855	0,42	0,44	1,6	0,36	381	86	0,22	453
	2860	0,42	0,24	1,26	0,36	300	86	0,16	448
	2865	0,51	0,37	1,39	0,46	273	90	0,21	445
	2870	0,63	0,36	1,76	0,49	279	78	0,17	438
	2875	0,62	0,33	1,67	0,54	269	87	0,16	439
	2880	0,65	0,28	1,75	0,47	269	72	0,14	440
	2885	0,77	0,48	2,36	0,57	306	74	0,17	439
	2890	0,91	0,5	3,38	0,52	371	57	0,13	443
	2895	0,7	0,64	2,46	0,54	351	77	0,21	442
	2905	0,59	0,48	2,05	0,46	347	78	0,19	442
	2910	0,77	0,55	2,75	0,49	357	64	0,17	439
	2920	0,7	0,38	2,35	0,44	336	63	0,14	442
	2925	0,8	0,49	3,09	0,37	386	46	0,14	441
2930	0,57	0,49	1,79	0,41	314	72	0,21	443	
2940	1,04	0,75	4,16	0,38	400	37	0,15	432	
2945	0,56	0,59	1,86	0,36	332	64	0,24	432	

4 Results and discussion

4.1 Gravity data analysis

The Bouguer contour map of the Jeffara basin and their surrounding areas reveals some spatially characteristic patterns. Distinction between these patterns is made based on the amplitudes of the anomalies. The Bouguer gravity anomaly (Fig. 5) varies from less than -25 mGal in the Permian Basin near Tataouine-Remada region to more than 11 mGal toward Tripolitania and Ashtart basins and five main anomalies labeled as GA1–GA5 are identified.

GA1 is a NW–SE-oriented positive anomaly exceeding 11 mGal and extending from the Jeffara basin in south-eastern Tunisia towards the Libyan promontory, to the east (Gabtni et al., 2009a, 2009b). GA2 is a major negative gravity anomaly matching with Tataouine basin extending overall Tataouine-Remada region in southern Tunisia, acknowledged as subsided area during Jurassic (Ben Ismail and M'rabet, 1990) with anomaly values less than -25 mGal. GA3 (0 to -2 mGal) is a positive gravity anomaly related to

the Precambrian Bounemcha uplift (Gabtni et al., 2009a, 2009b). GA4 is a negative gravity anomaly (-6 to -10 mGal) located within the Gulf of Gabes and Ashtart and Tripolitania basins. And GA5 (5 to 10 mGal) is NW–SE-oriented regional positive gravity anomaly that underlies the eastern margin of Tunisia and the Ashtart-Tripolitania basin in the Pelagian shelf. To attenuate the gravity effect of shallow geological bodies and to provide a crustal picture originating from deep sources of the Jeffara basin within their surrounding areas, we have applied the upward continuation of gravity field at 50 km altitude to compute the map of Fig. 5. This map reveals the regional gravity pattern of the "Crust—Upper Mantle" interface using the Jacobsen proposal for a sandwich source distribution.

The upward continuation map of the gravity field at 50 km in the study area (Fig. 6) shows that gravity anomalies trend mainly NW–SE. The main computed positive anomaly reaching 3.8 mGal is located within the Jeffara basin and exhibits an NW–SE oriented axis that passes southwestward Ezzaouia and El Bibane fields. This anomaly gradually decreases toward the west to ~0.8 mGal in

Table 3 Data used to generate burial-history curves for P2

Series, Unit, Event	Age (m.y)	Top depth (m)	Eroded (m)	Lithology
Actual	0	0		
Plio-Pleistocene	2			
<i>Unconformity</i>				
Oued Ben Khedim	5,5	95		Clay (75%), gypsum (25%)
Melquart	7	160		Clay (90%), gypsum (5%), lms (5%)
Beglia	9	250		ss (65%), clay (35%)
Mahmoud	13	330		Clay (90%), lms (5%) ss (5%)
Salambo	16,5	400		Clay (75%), lms (25%)
Upper Ketatna	20	790		lms (90%), clay (10%)
Lower Ketatna	22	1103		clay (90%), lms (10%)
Fortuna	24	1150		ss (75%), clay (10%), lms (5%)
Tanit	36	1169		dolomitic clay (95%), ss (5%)
<i>Unconformity</i>				
El Haria (<i>hiatus</i>)	55		100	marl
Abiod (<i>hiatus</i>)	65		100	lms
Upper Aleg	75	1453,5		clay (90%), lms (10%)
<i>intra-Aleg unconformity</i>				
Lower Aleg 1	77	1626,5		clay (80%) lms (20%)
Lower Aleg2	80	1735		marl
Douleb	84	1791		lms (80%), clay (20%)
Beida	89	2069		dol (65%), anh (35%)
Upper Zebbag (Gattar)	92	2238		dol anh
Middle Zebbag	94	2278		dol (85%), anh (10), clay (5)
Lower Zebbag	96	2350		dol anhy
<i>Austrian unconformity</i>			573	
Orbata (<i>hiatus</i>)	100		44	dol
Foum El Clayoub (<i>hiatus</i>)	112		12	clay
Barani (<i>hiatus</i>)	115		23	ss (60%), dol (40%)
Sidi Aïch (<i>hiatus</i>)	118		98	ss (65%), clay (35%)
Bou Hedma 1 (<i>hiatus</i>)	122		30	dol (80%), anhy (20%)
Bou Hedma 2 (<i>hiatus</i>)	125		366	ss (50%), clay (50%)
Bou Dinar	130	2423		ss clays
<i>Unconformity</i>				
Foum Tataouine	140	2534		dol (80%), clay (15%), sable (5%)
Mrabtime	145	2550		dol (35%), clay (35%), sable(15), anhy(15)
<i>Tlalett</i>	155	<i>Faulted</i>		
Smida	162	2785		clay (50%) dol (45%) ss (5%)
Krachoua	167	2842		dol (60%) anhy (25%) clay (15%)
Mestaoua	175	3025		anh (85%) clay (15%)
Horizon B	190	3265		dolomitic clay
Adjaj/Bhir	195	3275		lms -clay (50%) anhy (50%)

ss = sandstone, sh = shale, lms = limestone, anh = anhydrite, dol = dolomite, mr = marl

Tataouine basin home of negative anomaly. The gravity gradient between GA1 and GA2 is related to the buried Jeffara normal fault system (Ben Ayed, 1986; Bouaziz, 1995; Gabtni et al., 2009a, 2009b) associated to the Mesozoic rifting and engendering a general gradual slope and deepening toward the northwest. The GA5 reaches less

than -1.9 mGal in the Pelagian shelf alongside an area oriented mainly NW–SE that matches with the Ashtart-Tripolitania basin acknowledged as part of the troughs system restricted between Tunisia, Sicily and north of Tripolitania and resulted from the NE-SW Mesozoic extension of the eastern margin of Tunisia (Dhahri & Boukadi, 2017).

Table 4 Data used to generate burial-history curves for P3 well

Series, Unit, Event	Age (m.y)	Top depth (m)	Eroded (m)	Lithology
Actual	0	0		
Plio-Pleistocene	2	15,2		sh (60%) ss (35%), lms (5%)
<i>Pliocene Unconformity</i>			255	
Oued Ben Khedim (<i>Hiatus</i>)	5,5		95	sh (75%), gypsum (25%)
Melquart (<i>Hiatus</i>)	7		160	sh (90%), gypsum (5%), lms (5%)
Beglia	9	177		ss (80%), sh (20%)
Mahmoud	13	248		sh (65%), ss (25%), lms (10%)
Salambo	16,5	716		marlms
Upper Ketatna	20	778		lms
Lowe Ketatna	22	835		marlms
Fortuna	24	890		ss (50%), lms (25%), marls (25%)
Tanit	36	904		sh (50%), ss (40%), lms (10%)
<i>Unconformity</i>			373	
El Haria (<i>hiatus</i>)	55		100	marl
Abiod (<i>hiatus</i>)	65		100	lms
Upper Aleg (<i>hiatus</i>)	75		173	sh (90%), lms (10%)
<i>intra-Aleg Unconformity</i>			651,5	
Lower Aleg 1 (<i>hiatus</i>)	77		108,5	sh (80%) lms (20%)
Lower Aleg 2 (<i>hiatus</i>)	80		56	marls
Douleb (<i>hiatus</i>)	84		278	lms (80%), sh (20%)
Beida (<i>hiatus</i>)	89		169	anh (70%), dol (20%), sh 10%)
Upper Zebbag (<i>hiatus</i>)	92		40	dol (90%), anh 10%)
Middle Zebbag	94	963		dol
Lower Zebbag	96	1068		dol (75%), anhy (15%), sh (10%)
Orbata	100	1215		dol
Foum El Shoub	112	1269		shs
Barani	115	1281		ss (60%), dol (40%)
Sidi Aïch	118	1304		ss (65%), sh (35%)
Bou Hedma 1	122	1402		dol (80%), anhy (20%)
Bou Hedma 2	125	1430		ss (50%), sh (50%)
Bou Dinar	130	1800		ss
<i>Unconformity</i>				
Foum Tataouine	140	1944,5		dol (65%), anhy (20%), sh (10%), lms (5%)
Mrabtine	145	2188		dol (35), lms (35), sh (15), anh (10), ss (5)
Tlalett	155	2606,5		Dol
Smida	162	2730		dol (60%), lms (15%), sh (25%)
Krachoua	167	3010		Dol
Mestaoua	175	3130		dol (75%), lms (15%), anh (10%)
Horizon B	190	3325		Lmsaires
<i>Unconformity</i>				
Adjaj/Bhir	195	3340		dol (60%), anhy (40%)

ss = sandstone, sh = shale, lms = limestone, anh = anhydrite, dol = dolomite, mr = marl

To highlight and quantify the crustal thinning along the Jeffara area, a NE-SW density variation section (Fig. 7) was performed using inversion method. From SW to NE, this section reveals three main contrasting density bodies; a low-density body in Tataouine basin, a high-density body near

Ezzaouia and El Bibane fields related to a crustal thinning and delimited to the southwest by sharp vertical contours that match with the Jeffara fault, and an offshore moderate density body near the transition zone between the Jeffara and the Ashtart-Tripolitania basin. The crustal thinning effect

Table 5 Data used to generate burial-history curves for PF well

Series, Unit, Event	Age (m.y)	Top depth (m)	Eroded (m)	Lithology
<i>Post Vill. (Unconformity)</i>	0,8			
Segui	3			ss 80%, sh 20%
<i>Pliocene (Unconformity)</i>	5,5			
Oued bel khedim	6	150		sh 70%, anh 30%
Melquart	8	240		sh 70%,lms 20%, anh 10%
Beglia	15	350		ss 50%, sh 40%, lms 10%
Mahmoud	16	550		sh 65%, lms 25%, ss 10%
Ketatna	34	1000		sh 75%, lms 15%, ss 10%
<i>Oligocene (Unconformity)</i>	36			
Tanit	55	1435		sh 75%, lms 15%, ss 10%
<i>Santonien (Unconformity)</i>	83		200	
Upper Aleg (<i>hiatus</i>)	86		200	marlms 50%, sh 40%, lms 10%
Middle Aleg	89,5	1900		sh 45%, marl 40%, lms 15%
Lower Aleg	90,5	2300		lms 45, sh 30, dol 15, anh 10
Beida	91	2800		anh 70%, dol 20%, sh 10%
Guettar	91,5	2977		dol 90%, anh 10%
Zebbag	95	3030		dol 75%, anh 15%, sh 10%
<i>Albien (Unconformity)</i>	108		600	
Orbata/Sidi Aïch (<i>hiatus</i>)	125		600	sh 35, ss 25, dol 20, anh 10
Bou Dinar	130	3300		ss 80%, sh 10%, dol 10%
<i>Lw. Cretaceous (Unconformity)</i>	145			
Mrabtine	155	3420		dol 35, ss 25, sh 20, anh 20
Tlalett	160	3700		dol 75%, sh 15%, anh 10%
Smida	170	3800		sh 50, dol 20, ss 20, anh 10
Krachoua/Mestaoua	189	4050		dol 55%, anh 35%, sh 10%
Horizon B	192	4524		lms 50%, dol 50%
Bhir	225	4560		anh 50, dol 20, ss 10, sh 10
Rehach	227	5550		lms 50%, sh 30%, dol 20%
Azizia	232	5650		lms 50, sh 30, dol 10, ss 10
Kirchaou	237	6050		ss 80%, sh 20%

ss = sandstone, sh = shale, lms = limestone, anh = anhydrite, dol = dolomite, mr = marl

in the Jeffara basin and particularly around the Ezzaouia-El Bibane petroleum province (Fig. 2) is also characterized locally by a positive geothermal heat flow (Della Vedova, 1995; Gabtni et al., 2009a, 2009b).

Several surface heat-flow density (HFD) data have been used by Della Vedova et al. (1995) to obtain a HFD approximation for the tectonic provinces crossed by the southern segment of the European Geotraverse. In Tunisia and particularly in the Jeffara basin, we note the presence of HFD values generally higher than 100 mWm^{-2} . These types of values are classically observed in the rifting areas (Della Vedova et al., 1995). Oil and Gas of the Ezzaouia and El Bibane fields were generated in conjoint association with the thermal regime and the crustal context of the Jeffara basin. The regional structure of the Jeffara basin is directly related to an important crustal thinning revealed by gravity anomalies and large Permo-Triassic subsidence in Southern Tunisia. This subsidence is the consequence of the activity

of the northeast-dipping Jeffara normal faults system showed in Fig. 7 that highlights particular crustal thinning around the Ezzaouia-El Bibane petroleum district coupled with positive geothermal heat flow.

4.2 Petroleum system of the Jeffara basin

El Bibane, Ezzaouia and Robbana oil fields have been discovered to the south of Gulf of Gabes (Rodgers et al., 1990). In these fields hydrocarbons are trapped in a variety of reservoirs ranging from Upper Triassic to Upper Cretaceous in age. The Ezzaouia oil field consists of two productive intervals: the karst and fractured dolomites of Zebbag Formation (Upper Cretaceous) and the clastic Mrabtine member (Upper Jurassic). El Bibane tested oil and gas from Upper and Lower Zebbag dolomites, and gas condensate has been tested from the Krachoua (Jurassic). In Robbana field, oil is produced from Hauterivian sandy levels (Rodgers et al.

Table 6 Bottom Hole Temperature and vitrinite reflectance values used for calibration

Well	Depth (m)	BHT (°C)	Ro (%)
P1	833	–	0.36
	1379	–	0.46
	1435	83	–
	1692	–	0.52
	2058	–	0.58
	3148	121	–
	3489	127	–
P2	2205	99	–
	2337	105	1.8
	2742	–	0.84
	2767	–	1.82
	3128	–	1.39
	3248	124	–
	3268	132	–
PF	3818	494	1.43
	3854	495	1.47
	3890	496	1.51
	3925	497	1.55
	3961	498	1.59
	3997	500	1.63
	4032	502	1.66

1990). The main elements of the petroleum system are as follows:

The Source Rock: several organic rich levels were identified within the Jurassic and Lower Cretaceous series in the study area. Source-rock facies within the Jurassic series have been documented in surface as well as in subsurface in some wells from Central Tunisia, the Jeffara, the Chotts basins and in the Gulf of Gabes where the oil stored in the Mrabtime sandstones formation is thought to be derived from the Middle Jurassic organic-rich levels (Soussi, 2004). In the South of the Gulf of Gabes, the Smida member which is Callovian in age (Middle Nara) displays TOC values up to 12% and exhibit good petroleum potential up to 10 kg of HC/T of rock. The organic matter is mostly of type II kerogen (HI up to 394 mg of HC/g of TOC) and is marginally mature (Table 1).

The Rock–Eval pyrolysis of samples taken from the Smida source rock between –2842 and –2784 m in the P2 well (Table 2) show TOC values between 0.31 and 0.42%. The HI vs OI diagram (Fig. 8a) shows that the organic matter is mostly of type III kerogen (HI up to 100 mg of HC/g of TOC). Tmax values range between 432 °C and 445 °C and production index values (0,18 to 0,2) are indicative of

oil window stage. In P3 well (Table 2) TOC values range between 0.42 and 1.06%. The HI vs OI diagram (Fig. 8b) shows that the organic matter is mostly of type II and type III kerogens as indicated by HI up to 390 mg of HC/g of TOC. The Tmax values obtained from Rock–Eval pyrolysis for P2 and P3 (Table 2) range from 432 to 453 °C and they are mostly indicative of mature organic matter classify the Smida member as the main source rock.

Reservoirs and Seals: The Upper Jurassic deltaic to coastal marine sandstones bodies of the Mrabtime member exhibit good reservoir qualities with a porosity of 17% and a permeability of 130 md (values considered for the EZZ 2 well). The average porosity is of more than 15%, and permeability is up to several Darcies. The Mrabtime reservoir is sealed by the Tithonian evaporates. However, hydrocarbons originated from the Middle Jurassic organic-rich shale and mudstone deposited underneath.

4.3 Burial history modelling

The burial history reconstruction using P3 data (Fig. 9) shows that during Mid-Upper Jurassic to Early Cretaceous (from –160 to –110 million years (m.y)) subsidence/sedimentation rates increased with an average rate of 35 m/Ma. This phase of subsidence is correlated to the Tethyan rifting related to the breakup of Gondwana, which has been documented in many previous studies throughout the Tethyan margin (Dercourt et al., 2000; Dhahri & Boukadi, 2017; Gabtni et al., 2013; Guiraud, 1998). Between -110 and -100 m.y (series D in Fig. 7) the subsidence recorded a cease; in fact, this interval corresponds to the Aptian–Albian transition characterized in central and southern Tunisia by a sea level fall and an unconformity between Aptian and Albian series with local erosion and/or no deposition records (Marco et al., 2014). After this cease, deposition took back near P3 and seems to be sustained until about –60 m.y then disturbed by a Paleocene-Eocene event lasting to about –55 m.y and engendered an erosion during the following 25 m.y that removed approximately 600 m of sediments prior to renewed deposition of post-Miocene units. The Smida source rock was buried at about 1400 m during Aptian (–110 m.y) in P3 but it reached 2100 m in P2 during the same period which argues relatively for the subsidence of the area near P3. The rate of deposition increased substantially between Cenomanian and Coniacian period (–86 m.y) and accumulated more than 3200 m of marine sediments. However, after –80 m.y the curves in Fig. 9 tend to be less steep indicating a subsidence decrease tendency. This is subsequent to a prior extensional tectonic that occurred between -83 and –80 m.y (Campanian time) and that created

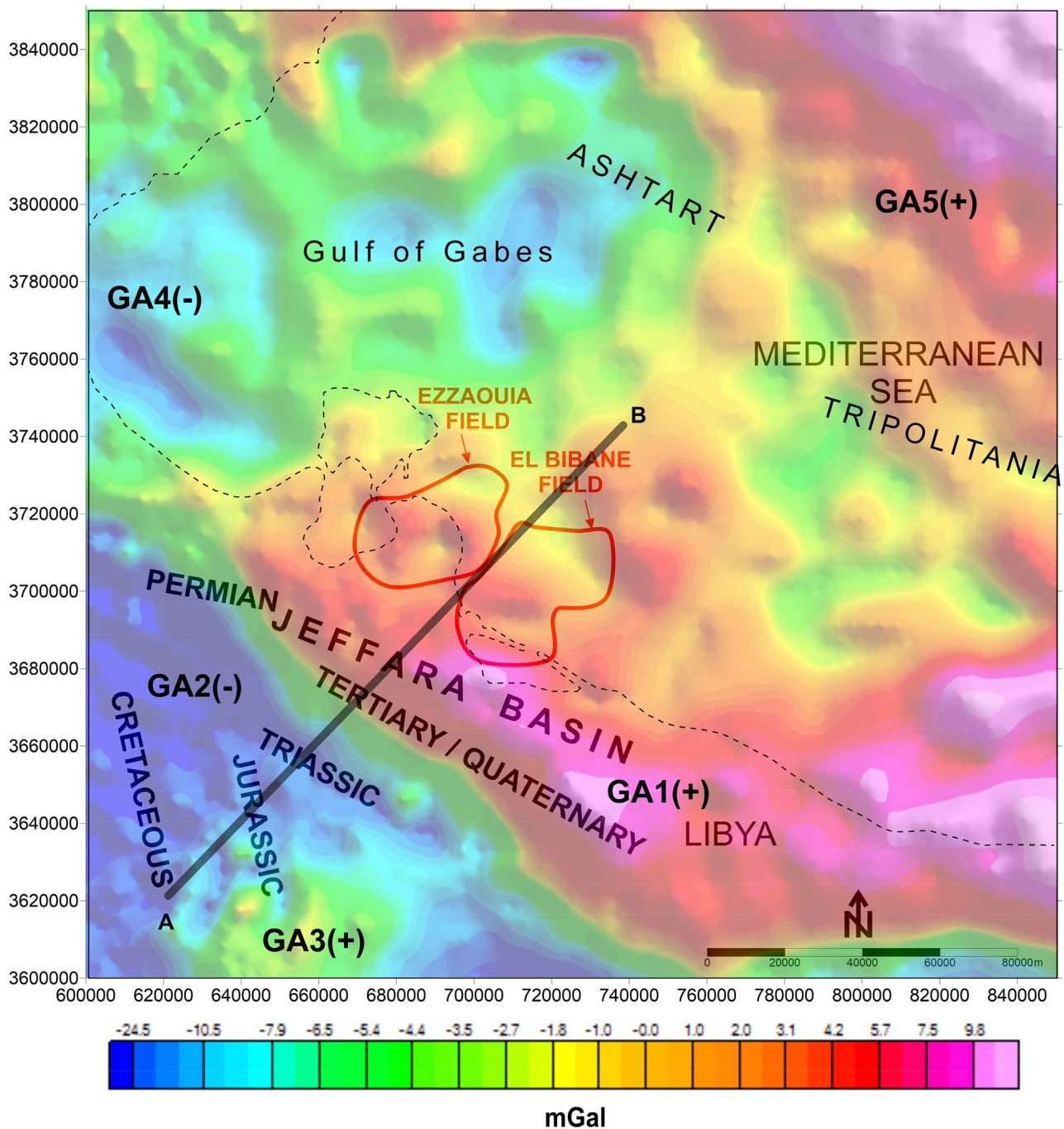


Fig. 5 Bouguer gravity map of the study area. GA1–GA5 are the gravity anomaly, (+)/(-) indicate the positive/negative character of the anomaly, the thin black dashed line indicates the shore line, A–B line locates the section of Fig. 7

an uplifted block near P3 that experienced erosion of an estimated thick of ~ 1000 m of sediments. Between Paleogene and Miocene, the rate of deposition increased substantially

(subvertical curves, Fig. 9) with an average ~ 40 m/m.y during the Pliocene leading to deposition of ~ 3300 m thick sequence.

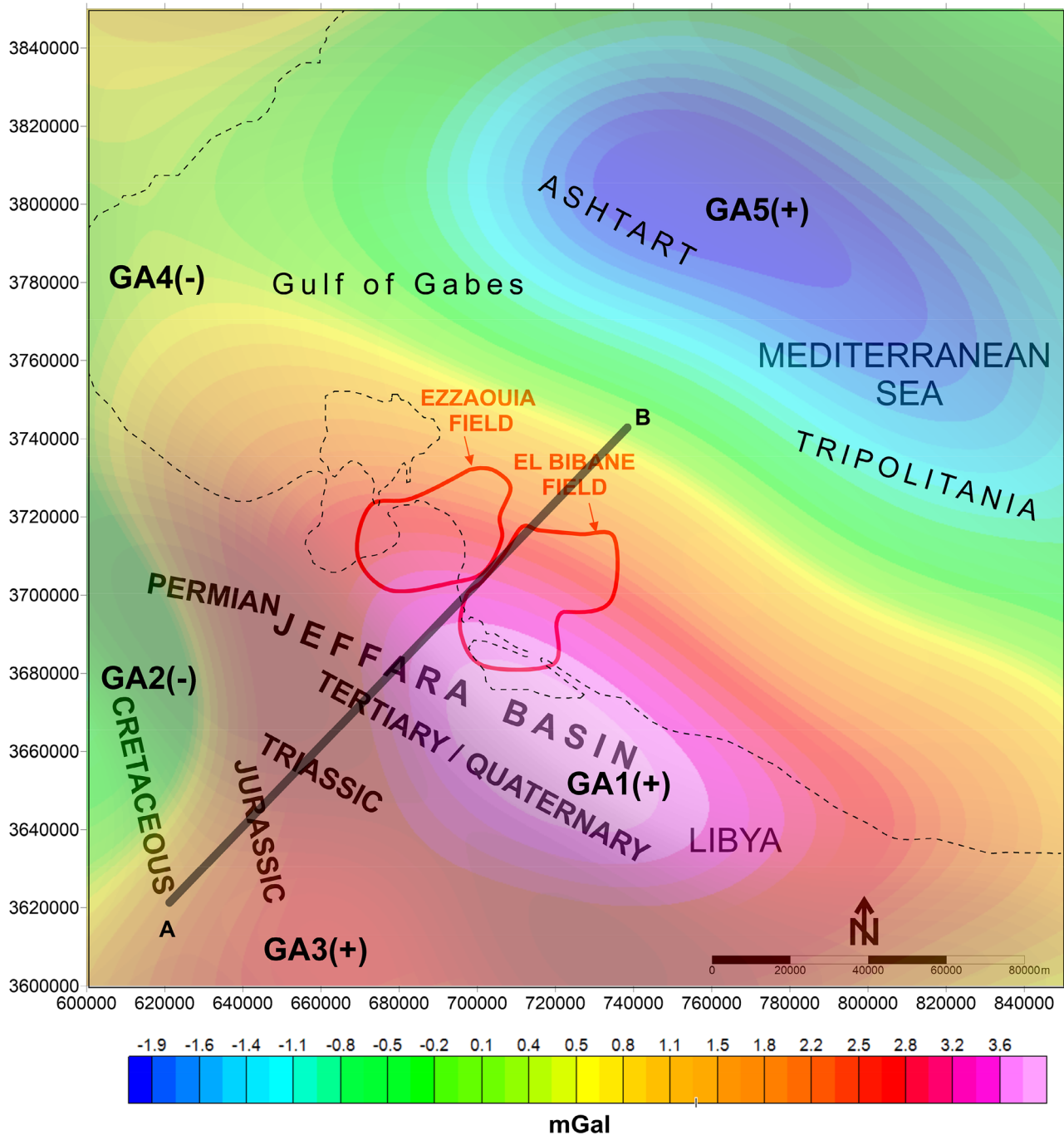


Fig. 6 Upward continuation map of the gravity field at 50 km in the study area. Same legend as in Fig. 5

The burial history reconstructed for P2 (Fig. 10) is a bit similar to that of P3 however, the sediment accumulation rate during the Jurassic-Cretaceous period is relatively low with a cumulated thickness of ~2,4 km at the end of Cretaceous

(Fig. 10) versus ~3,6 km in P3 (Fig. 9). The burial rate was about 20 m/m.y. The rise of Smida Formation from a depth of 1000 m (–110 m.y) to 500 m (–100 m.y) is subsequent to the Aptian Austrian tectonic event engendering the creation

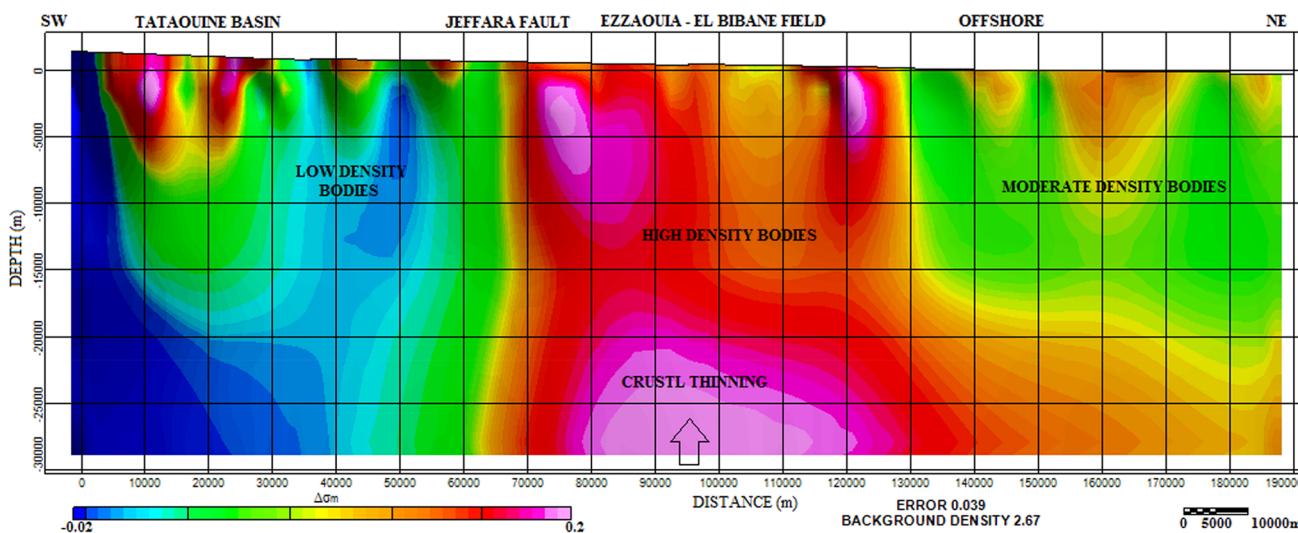


Fig. 7 A–B SW-NE-oriented density variation section showing a particular crustal thinning around the Ezzaouia-El Bibane petroleum fields (Location on Figs. 2, 5 and 6). Unit: density contrast in g/cm^3

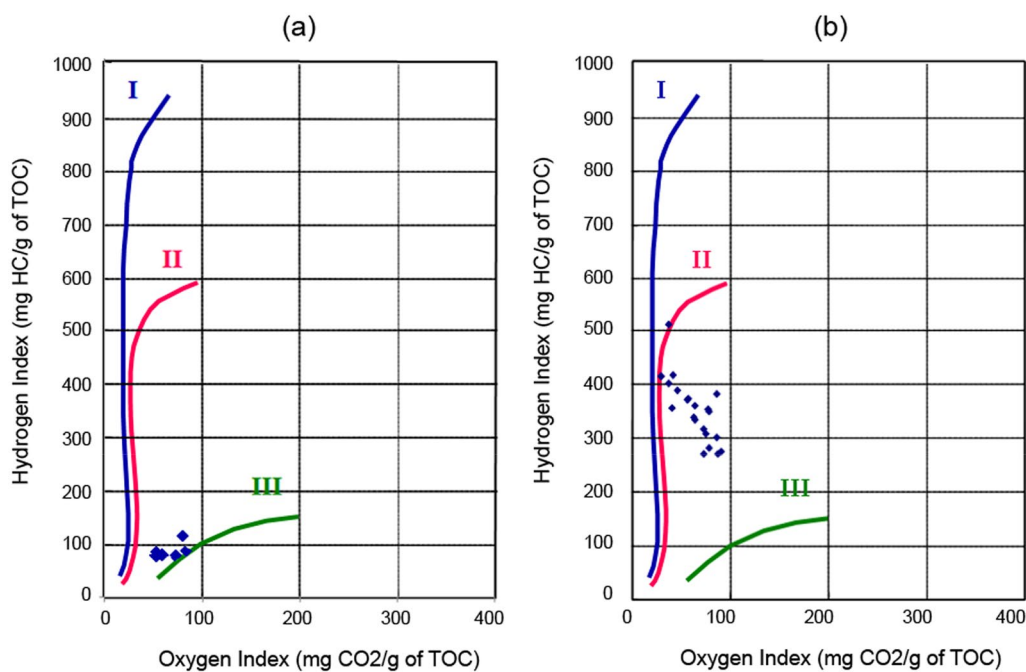


Fig. 8 HI vs OI diagrams based on Rock–Eval pyrolysis results of P2 (a) and P3 (b) wells

of low and high blocks in the Tunisian domain. The role of erosion of the uplifted blocks should not be neglected in the thickness decrease of Upper Cretaceous and following

series. From -100 to -60 m.y, the burial-history curves exhibit the same tendency of these in P3. The rate of deposition estimated for the Paleogene-Miocene period indicate

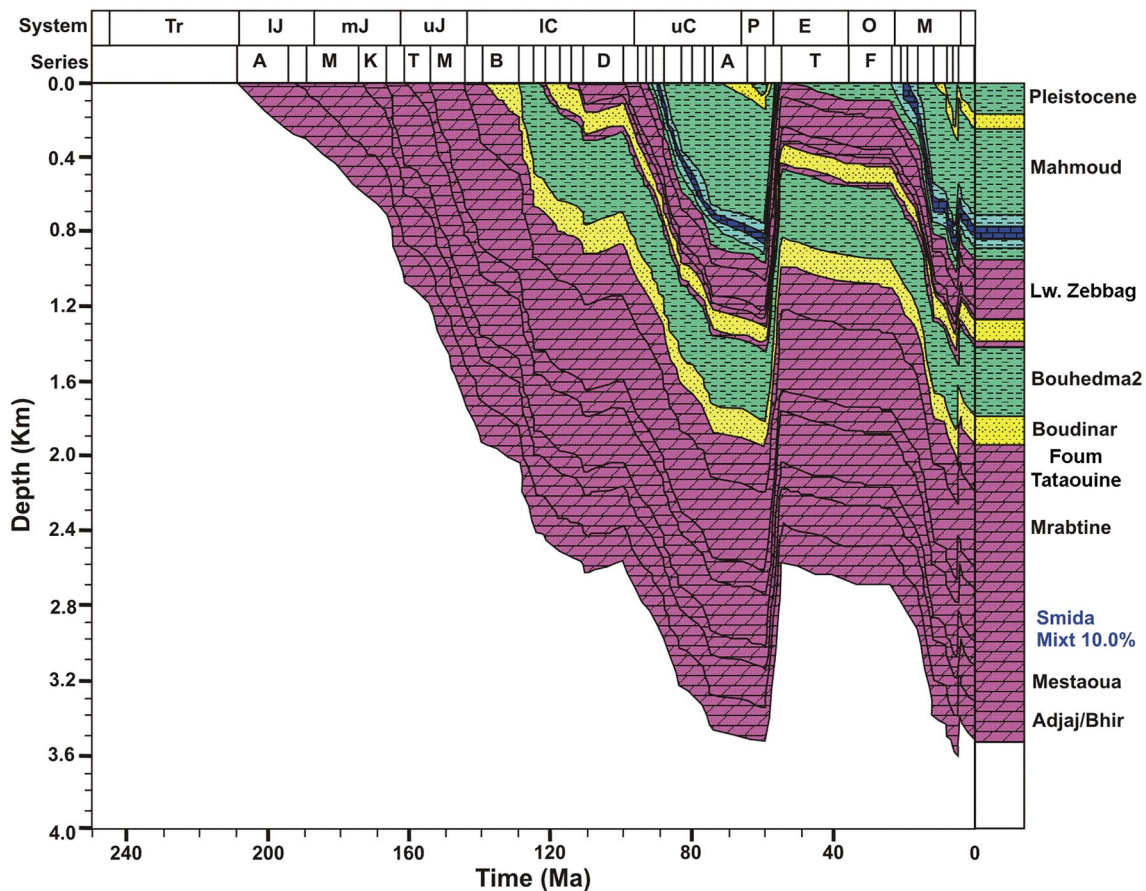


Fig. 9 Burial history curve at the gulf of Gabes location (well P3). Used data are of Table 4

a subsidence increase such in P3 and exhibits the same average of about 40 m/m.y during the Pliocene.

The burial history established for the pseudo-well PF (Fig. 11) gives the opportunity to observe the basin evolution during overall the Mesozoic era. During Triassic and Jurassic, burial values are significant and exhibit an average of 26 m/m.y. From uppermost Jurassic to earliest Cretaceous (–145 to –130 m.y), the horizontal curves in Fig. 11 indicate no subsidence (series C) locally near PF well due to the Jurassic/Cretaceous unconformity. The Cenomanian–Turonian period is marked by very high values of subsidence (subvertical curves) with deposition buried to about 1600 m depth. Between -85 and -55 m.y curves are inverted which can be correlated to the uplift of the area subsequent to the Upper Cretaceous tectonics. And during Eocene-Miocene period values of subsidence are of 17 m/m.y in average with a significant Middle Miocene increase near –15 m.y.

4.4 Thermal modelling

Thermal calibrations carried out for P1, P2 and P3 wells using Genex software showed that the best adjustments between the measured and calculated values were obtained for a heat flux varying between 60 and 65 mW/m². Figure 12 shows the calibration plots of P1 based on BHT (Fig. 12a), Rock–Eval Temperature (Fig. 12b) and vitrinite reflectance (Fig. 12c).

The evolution of the heat flow of the area is conditioned by the tectonic activity in the region and it is optimized by reducing the differences between measured and calculated temperature and the reflectance of vitrinite. Yukler et al. (1995) showed that the values of the heat flow increase from the Callovian to the Late Jurassic and keeps their high values 8 m.y before the gradual decline that occurred between the Lower and Middle Aptian to reach a stable value.

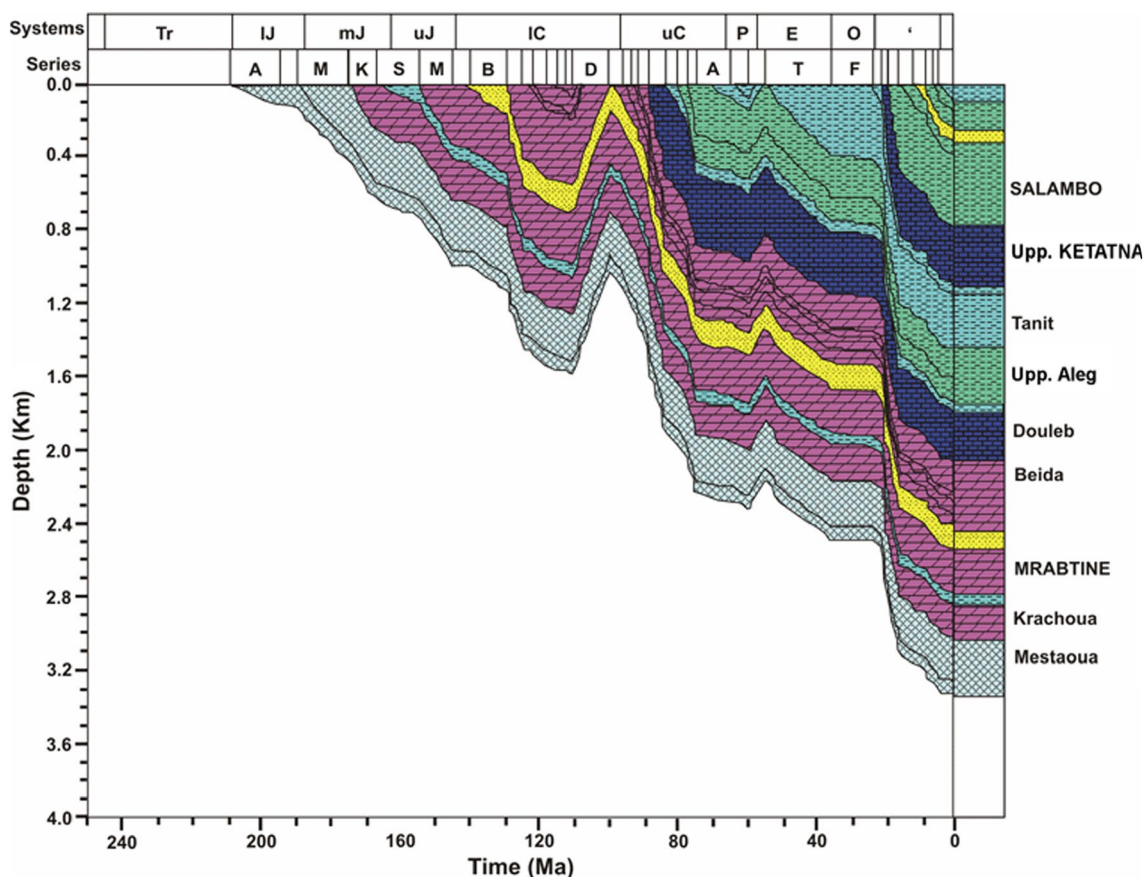


Fig. 10 Burial history curve at the gulf of Gabes location (well P2). Used data are of table

The heat flow begins to increase at the Upper Albian and Cenomanian then gradually decreases to stabilize at the Paleocene and keeps that value until the Langhian (–17 m.y).

From the Langhian, a gradual increase in heat flow is recorded until Tortonian average (–9 m.y) followed by a sharp increase until the Pliocene (–3 to –2 m.y) where the highest values of heat flow were recorded. The values of the heat flow begin to decrease during the last 2 m.y, but they are far from reaching stability; the last increase of the heat flux in the Pliocene is considered the most important factor leading to the generation of hydrocarbons in the Gulf of Gabes region.

The thermal history has followed a similar trend in the different wells that can be divided into four cycles where each cycle shows a period of warming and a cooling period. Cooling may have been caused by uplift and erosion, or heat flow decline. In terms of thermal maturity, the source rock of Smida Formation has recorded two main phases: the first phase of warming occurred over the Lower Cretaceous between Austrian and Santonian compression (Fig. 13). This

warming phase has contributed to the hydrocarbon generation in P3 well. The second phase which is recorded in the Paleogene led to the hydrocarbon generation and expulsion in P2 and PF wells. Figure 13 show the events chart of the petroleum system evolution in the study area. It exposes the oil/source correlation study should be of the Mrabtine and Zebbag reservoirs.

4.5 Hydrocarbon maturation

The source rock maturity and hydrocarbon generation modelling results are presented in Fig. 14. The geo-history plot of P2 well (Fig. 14a) indicates that the Smida source rock evolved to the oil window at ~ –108 m.y with a maximum reached at Miocene (–25 m.y). It evolved to wet gas window during Coniacian near –80 m.y. The generation of oil and gas through time for the source rocks in P2 well (Fig. 14b) was calculated using standard techniques and compositional kerogen kinetics. The Fig. 14b shows that some oil and minor gas were expelled during Langhian (–15 m.y) and

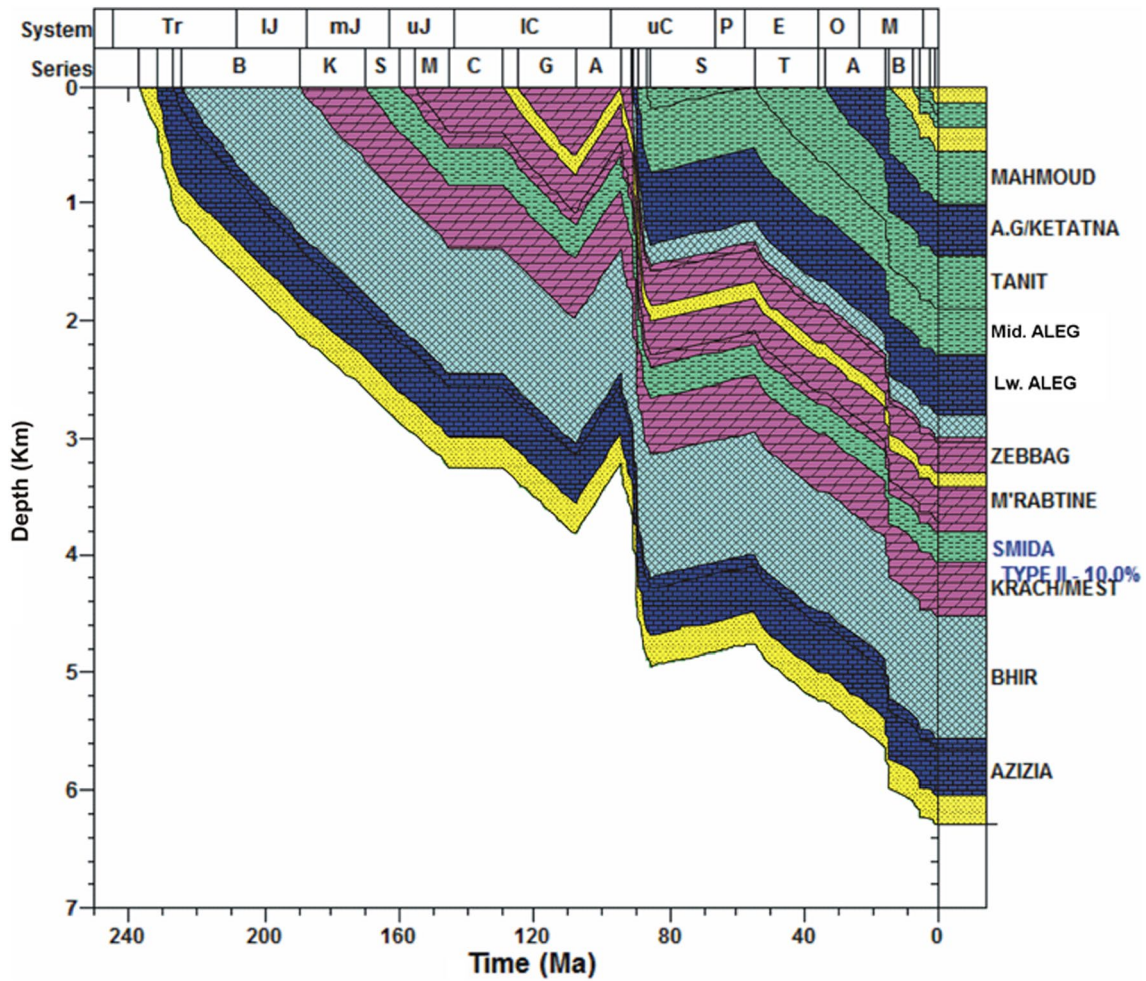


Fig. 11 Burial history curve at the Gulf of Gabes (well PF). Used data are of Table 5

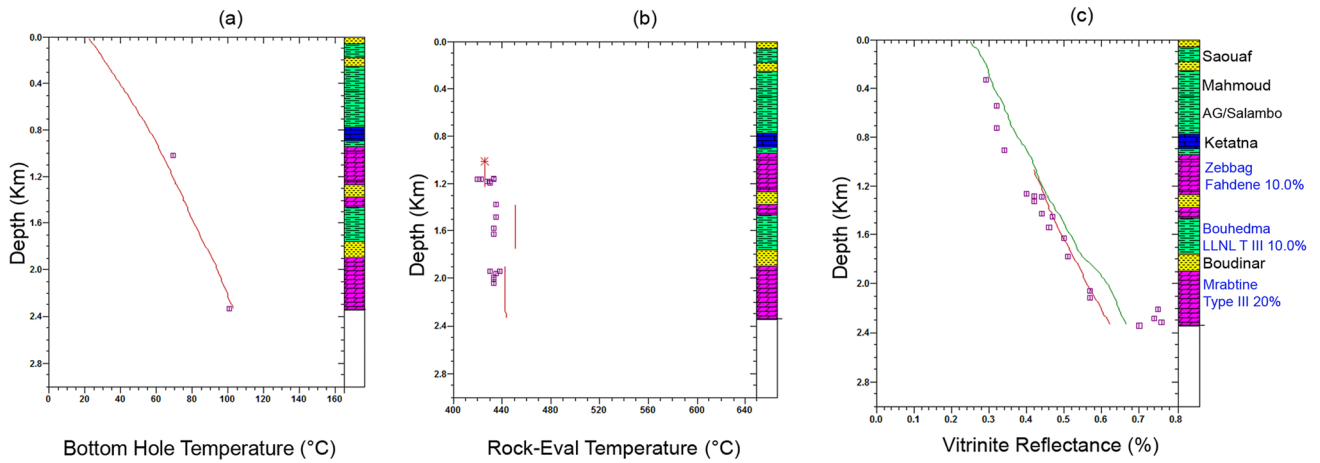


Fig. 12 Calibration plot of P1 well based on Bottom Home Temperature (a), Rock–Eval Temperature (b) and vitrinite reflectance (c)

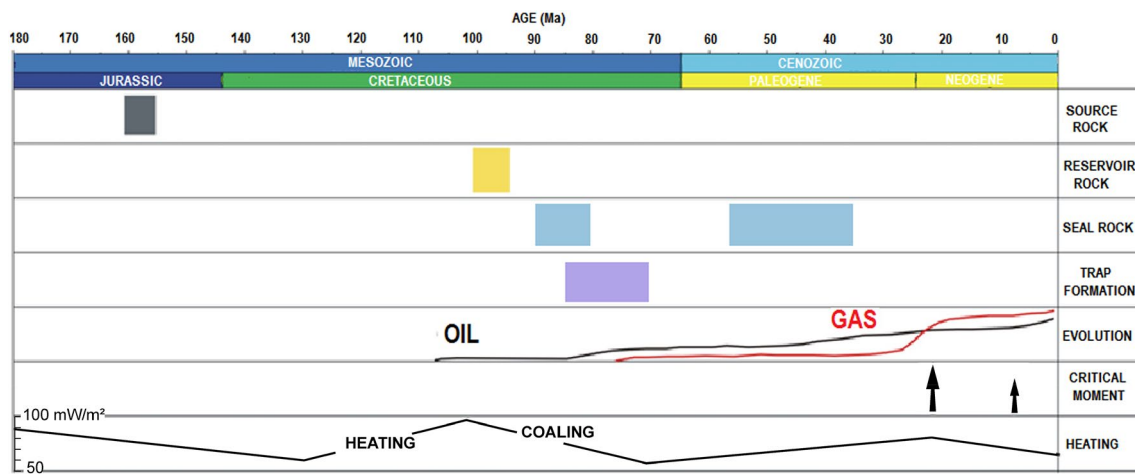


Fig. 13 Events chart of the petroleum system evolution in the study area

continued until the Early Tortonian (–10 m.y). Figure 14c shows that the Smida source rock in the P3 well reached the oil window since the Early Cretaceous (–140 m.y) and gas window only from the Coniacian (–80 m.y). The largest quantities of hydrocarbons were generated from the Langhian (–15 m.y) until the present day without reaching the maximum generation phase. The Jurassic source rock of Smida Formation has not expelled hydrocarbon since it has not reached the saturation threshold (SATEX = 10%), defined as the amount of hydrocarbons beyond which the excess of oil produced is expelled from the rock.

The plot established for the pseudo-well PF (Fig. 14d) seems a bit similar to the P2 one. The Smida source rock reached the oil window at ~110 m.y and the gas window at Coniacian (–80 m.y). It reached the wet gas-condensate stage at Langhian (–15 m.y). The Fig. 9 shows that oil and gas were expelled during Middle Eocene (–45 m.y) and later to with a major expulsion during the Middle Oligocene (–30 m.y).

The interpretation of the burial history curves pointed out four main subsidence phases between Jurassic and the present time. The first phase is related to the Tethyan rifting resulting from the breakup of Gondwana documented in several previous studies throughout the Tethyan margin (Dercourt et al., 2000; Dhahri & Boukadi, 2017; Gabtni et al., 2013; Guiraud, 1998). This phase is characterized by relatively high burial rates estimated to 35 and 25 m/m.y in P3 and P2 wells respectively. This subsidence was interrupted by the Austrian event at the end of Lower Cretaceous. The local uplift of the Ezzaouia area resulted in the initiation of basin inversion. The second phase of subsidence occurred during the Upper Cretaceous. It was

characterized by fast and significant increase in subsidence during Cenomanian–Turonian times however near the Santonian, P2 and P2 curves show a relative decrease in subsidence related to the Late Santonian compression (Guiraud & Bosworth, 1997). This decrease will be more obvious for the Campanian–Paleocene period. Conversely the curves of Fig. 9 argue for erosion near PF well from Santonian to Early Eocene. The Cenozoic compressional tectonics was responsible for the formation of NE–SW trending folds in the Atlasic domain and contemporaneous NW–SE oriented diapirs and salt walls. Subsequent erosion may occur within resulted reliefs such Ezzaouia and El Bibane folds. During Cenozoic, Ezzaouia area was relatively the heist area which resulted in the erosion of about 1000 m from Upper Cretaceous (Abiod Formation) and Paleocene (Harria Formation) sediments in P3 (Table 4). This erosion affected also the area near P2 well (considered relatively in low position) and it was less intensive there since it eroded only 200 m. During Eocene–Oligocene period, subsidence/sedimentation took back with an estimate rate of 8 m/m.y. During Miocene–Pliocene period, the rate of deposition increased substantially with an average of 40 m/m.y in the Pliocene and led to the accumulation of 3300 m of sediments. This subsidence corresponds to the Miocene NE–SW extension related to the reactivation of inherited NW–SE trending faults as normal faults. Later on, the NW–SE Villafranchian compression (–4 m.y) enhanced the deformation of the NE–SW Cretaceous folds. In addition, halokinetic movements are responsible for some local deformations and structure complexity.

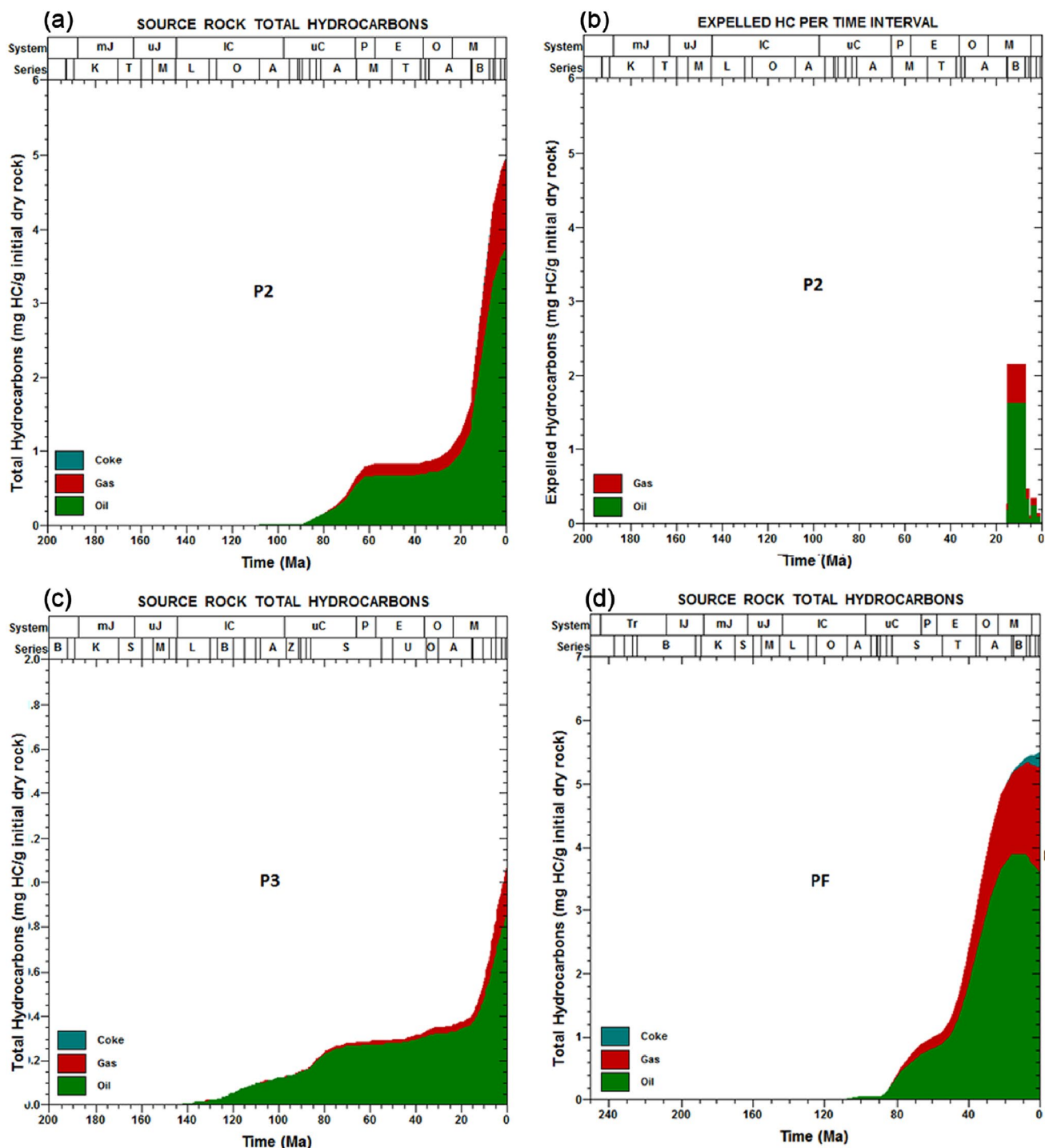


Fig. 14 Hydrocarbon generation/expulsion from the source rock of Smida in the studied wells

Regarding the generation and expulsion of hydrocarbons from the Smida source rock, geochemical analyses have shown that sediments of this formation have reached the oil window in the P2, P3 and PF wells with different origins (terrestrial in P2 and mixed in P3). The hydrocarbon generation started from the Lower Cretaceous in

P3 well and from the mid-Cretaceous in P2 well and PF pseudo-well. The Smida source rock was able to generate greater amounts of hydrocarbon in P2 well and then in PF, however in P3 well hydrocarbon generation do not exceed 1 mg HC/g, which does not reach the saturation threshold (SATEX) (Fig. 10).

The thermal conditions experienced by the study area allowed the expulsion of hydrocarbons from Smida source rock at P2 and PF wells. This source rock is considered the main candidate source that fed the Zebbagg reservoir at P2 and P3 wells.

5 Conclusion

The gravity data analysis using inversion method shows that the Jeffara basin in southeastern Tunisia is associated with a regional major NW–SE positive gravity anomaly related to about 5 km crustal thinning from west to East. This crustal thinning setting have locally controlled the burial and heat flow histories of Ezzaouia and El Bibane oil fields. The region is configured into two main tectonic provinces corresponding to the Ezzaouia area in the North and El Bibane area in the South, separated by the tectonic boundary of the Jeffara fault. The cumulative offsets of the NW–SE trending segments of the Jeffara fault system during the rifting periods engendered the extension and the thinning of the affected crust near the Jeffara area and Ashtart-Tripolitania basin which resulted also in a positive geothermal heat flow. The heat flow chart shows two main phases of warming. The first occurred in Lower Cretaceous and engendered hydrocarbon generation in Ezzaouia field, whereas, the second occurred in Paleogene and led to the hydrocarbon generation and expulsion in El Bibane field.

The burial history reconstruction of the Ezzaouia-El Bibane area for Mesozoic-Cenozoic times shows periods of increase and decrease of subsidence with local erosion. Jurassic-Cretaceous period is mainly period of increased subsidence/sedimentation rates with an average rate of 35 m/m.y. but concerned by an interval of subsidence cease during the Aptian–Albian transition also associated to local erosion. The Paleocene-Eocene was a period of subsidence cease followed by erosion. During Mid-Miocene-Pliocene the rate of deposition increased substantially and led to deposition of thick sequence. These period of contrasted subsidence/deposition rates are correlated to the acknowledged tectonic events that affected the study area.

Acknowledgements We are thankful to the "Bureau Gravimétrique International" (BGI) for the support and the access to satellite gravity data and also the "Entreprise Tunisienne d'Activités Pétrolières" (ETAP) for access to wells data. We thank also Pr. Javier Martin-Chivilet, the Editor in Chief of the Journal of Iberian Geology, Dr. Silvia Omodeo Salé and the other anonymous reviewers for their valuable and constructive comments that helped us to improve the manuscript.

Funding Not applicable.

Availability of data and materials Satellite gravity data are provided by the "Bureau Gravimétrique International" (BGI). Well data are provided by the "Entreprise Tunisienne d'Activités Pétrolières" (ETAP).

Declarations

Conflict of interest The authors declare that they have no competing interests.

Ethics approval Not applicable.

Consent to participate All the authors declare that they agree to co-authors the manuscript.

References

- Ben Ayed, N. (1986). *Evolution tectonique de l'avant pays de la chaîne alpine de Tunisie du début du Mésozoïque à l'Actuel*. University of Paris Sud, Paris.
- Ben Ferjani, A., Burolet, P., & Mejri, F. (1990). *Petroleum geology of Tunisia*. Entreprise Tunisienne d'Activités Pétrolières, Tunis.
- Ben Ismail, M. H., & M'Rabet, A. (1990). Evaporite, carbonate, and siliciclastic transitions in the Jurassic sequences of southeastern Tunisia. *Sedimentary Geology*, 66(1–2), 65–82.
- Benton, M. J., Bouaziz, S., Buffetaut, E., Martill, D., Ouaja, M., Soussi, M., & Trueman, C. (2000). Dinosaurs and other fossil vertebrates from fluvial deposits in the Lower Cretaceous of southern Tunisia. *Palaeogeography, Palaeoclimatology, Palaeoecology*, 157(3–4), 227–246.
- Bishop, W. F. (1975). Geology of Tunisia and adjacent parts of Algeria and Libya. *American Association of Petroleum Geologists Bulletin*, 59, 413–450.
- Bodin, S., Petitpierre, L., Wood, J., Elkanouni, I., & Redfern, J. (2010). Timing of early to mid-cretaceous tectonic phases along North Africa: New insights from the Jeffara escarpment (Libya–Tunisia). *Journal of African Earth Sciences*, 58(3), 489–506.
- Booth-Rea, G., Gaidi, S., Melki, F., Marzougui, W., Azañón, J. M., Zargouni, F., Galvé, P., & Pérez-Peña, J. V. (2018). Late Miocene extensional collapse of northern Tunisia. *Tectonics*, 37(6), 1626–1647.
- Bouaziz, S. (1995). *Etude de la tectonique cassante dans la plate-forme et l'Atlas saharien (Tunisie méridionale): évolution des paléochamps de contraintes et implications géodynamiques*. University of Tunis El Manar II, Tunis.
- Bouaziz, S., Barrier, E., Soussi, M., Turki, M. M., & Zouari, H. (2002). Tectonic evolution of the northern African margin in Tunisia from paleostress data and sedimentary record. *Tectonophysics*, 357, 227–253.
- Bouaziz, A., Mabrouk-El Asmi, A., Skanji, A., & El Asmi, K. (2015). A new borehole temperature adjustment in the Jeffara Basin (southeast Tunisia): Inferred source rock maturation and hydrocarbon generation via one-dimensional modeling. *American Association of Petroleum Geologists Bulletin*, 99, 1649–1669.
- Busson, G. (1967). *Le Mésozoïque Saharien, 1ère partie: l'extrême Sud Tunisiens*, Paris: C.N.R.S., 194 p
- Della Vedova, F., Lucazeau, V., Pasquale, G., & Pellis Verdoya, M. (1995). Heat flow in the tectonic provinces crossed by the southern segment of the European Geotraverse. *Tectonophysics*, 244, 57–74.
- Dercourt, J., Gaetani, M., & Vrielinck, B. (2000). Atlas Peri-Téthys and explaining notes (S. Crasquin coord). *Commission for the Geologic Map of the World Edition*, Paris.
- Dhahri, F., & Boukadi, N. (2017). Triassic salt sheets of Mezzouna, Central Tunisia: New comments on Late Cretaceous halokinesis and geodynamic evolution of the northern African margin. *Journal of African Earth Sciences*, 129, 318–329.

- Espitalié, J., Laporte, J. L., Madec, M., Marquis, F., Leplat, P., Paulet, J., & Boutefeu, F. (1977). Méthode rapide de caractérisation des roches mères, de leur potentiel pétrolier et de leur degré d'évolution. *Rev. Inst. Français Du Pétrole*, 32, 23–42.
- Espitalié, J., Deroo, G., & Marquis, F. (1985). La pyrolyse RockEval et ses applications : Part1. *Rev. Inst. Français Du Pétrole*, 40, 563–578.
- Fullea, J., Fernandez, M., & Zeyen, H. (2008). FA2BOUG-A FORTRAN 90 code to compute Bouguer gravity anomalies from gridded free-air anomalies: Application to the Atlantic-Mediterranean transition zone. *Computers & Geosciences*, 34, 1665–1681.
- Gabtni, H., Jallouli, C., Mickus, K. L., Zouari, H., & Turki, M. M. (2009a). Deep structure and crustal configuration of the Jeffara basin (Southern Tunisia) based on regional gravity, seismic reflection and borehole data: How to explain a gravity maximum within a large sedimentary basin? *Journal of Geodynamics*, 47, 142–152.
- Gabtni, H., Jallouli, C., Mickus, K. L., Zouari, H., & Turki, M. M. (2009b). Deep structure and crustal configuration of the Jeffara basin (Southern Tunisia) based on regional gravity, seismic reflection and borehole data: How to explain a gravity maximum within a large sedimentary basin? *Journal of Geodynamics*, 47(2–3), 142–152.
- Gabtni, H., Jallouli, C., Mickus, K. L., & Turki, M. M. (2013). Geodynamics of the Southern Tethyan Margin in Tunisia and Maghreb domain: New constraints from integrated geophysical study. *Arabian Journal of Geosciences*, 6(1), 271–286.
- Ghedhoui, R., Deffontaines, B., & Rabia, M. C. (2016). Neotectonics of coastal Jeffara (southern Tunisia): State of the art. *Tectonophysics*, 676, 211–228.
- Guiraud, R. (1998). Mesozoic rifting and basin inversion along the northern African Tethyan margin: An overview. *Geological Society, London, Special Publications*, 132(1), 217–229.
- Guiraud, R., & Bosworth, W. (1997). Senonian basin inversion and rejuvenation of rifting in Africa and Arabia: Synthesis and implications to plate-scale tectonics. *Tectonophysics*, 282(1–4), 39–82.
- Klett, T.R. (2001). Total Petroleum Systems of the Pelagian Province, Tunisia, Libya, Italy, and Malta-The Bou Dabbous-Tertiary and Jurassic-Cretaceous Composite. *US Department of the Interior, US Geological Survey*, Reston, 27, <https://doi.org/10.3133/b2202D>.
- Lazzez, M., Ben Rabah, R., & Maazaoui, A. (2014). Lower cretaceous petrophysical reservoir evaluation and petroleum prospectivity in the Jeffara basin (SE Tunisia). *Standard Global Journal of Geology and Explorational Research*, 1, 1–8.
- Marco, I., Dhahri, F., Haji, T., & Boukadi, N. (2014). Aptian-Albian transition in central Tunisia: Tectonosedimentary and paleogeographic records. *Journal of Earth Science*, 25(5), 787–798.
- Patriat, M., Ellouz, N., Dey, Z., Gaulier, J. M., & Ben Kilani, H. (2003). The Hammamet, Gabes and Chotts basins (Tunisia): A review of the subsidence history. *Sedimentary Geology*, 156, 241–262.
- Pavlis, N.K., Holmes, S.A., Kenyon, S.C., & Factor, J.K. (2008). An Earth Gravitational Model to Degree 2160: EGM2008. *EGU General Assembly*, Vienna, April 13–18, 2008.
- Raulin, C., de Lamotte, D. F., Bouaziz, S., Khomsi, S., Mouchot, N., Ruiz, G., & Guillocheau, F. (2011). Late Triassic–early Jurassic block tilting along E-W faults, in southern Tunisia: New interpretation of the Tebaga of Medenine. *Journal of African Earth Sciences*, 61(1), 94–104.
- Roberts, L. N., Lewan, M. D., Finn, T. M. (2005). Burial history, thermal maturity, and oil and gas generation history of petroleum systems in the southwestern Wyoming province, Wyoming, Colorado, and Utah. US Geological Survey Southwestern Wyoming Province Assessment Team, eds., Petroleum systems and geologic assessment of oil and gas in the southwestern Wyoming province, Wyoming, Colorado, and Utah: US Geological Survey Digital Data Series DDS-69-D, 25
- Rodgers, M. R., Beahm, D. C., Touati, M. A. (1990). Discovery of the Ezzaouia and Robbana Accumulations, Gulf of Gabes, Tunisia. AAPG Bulletin (American Association of Petroleum Geologists);(USA), 74, CONF-900605.
- Soussi, M., Fakhfakh-Ben Jemia, H., & Saidi, M. (2004). Jurassic Play in Southern Tunisia. *The 9th Tunisian petroleum exploration and production conference (Field trip book)*, Entreprise Tunisienne d'Activités Pétrolières, Tunis.
- Sweeney, J. J., & Burnham, A. K. (1990). Evaluation of a simple model of vitrinite reflectance based on chemical kinetics. *American Association of Petroleum Geologists Bulletin*, 74, 1559–1570.
- Touati, M. A., & Rodgers, M. R. (1998). Tectono-stratigraphic history of the southern gulf of Gabes and the hydrocarbon habitats. *Proceedings of the Sixth Tunisian Exploration and Production Conference*, Tunis, May 5–9, p. 343–370.
- Yukler, M. A., Moumen, A., & Daadouch, I. (1995). Quantitative evaluation of the geologic evolution and hydrocarbon potential of the Gulf of Gabes. *American Association of Petroleum Geologists Bulletin*, 1995, CONF-950995.